Electronic Supplementary Information

Regulation of electronic structure of RuNi/MoC electrocatalyst for high-efficiency hydrogen evolution in alkaline seawater

Xiaocheng Fan,[a] Bei Li,[b] Chunling Zhu,*[a] Feng Yan,*[b] and Yujin Chen*[a,b]

[a] Laboratory of Superlight Materials and Surface Technology, Ministry of Education, College of Materials Science and Chemical Engineering, Harbin Engineering University, Harbin 150001, China
E-mail: zhuchunling@hrbeu.edu.cn

[b] College of Physics and Optoelectronic Engineering, Harbin Engineering University, Harbin 150001, China
E-mail: chenyujin@hrbeu.edu.cn

This Supporting Information includes:
Experimental Section
References
Figures S1-S15
Tables S1-S6

1. Experimental section

1.1 Materials and Reagents

Ethanol, sodium molybdate dihydrate ($Na_2MoO_4 \cdot 2H_2O$, 98%), dicyandiamide (98%), nickel nitrate hexahydrate ($Ni(NO_3)_2 \cdot 6H_2O$, 98%), iron nitrate hexahydrate ($Fe(NO_3)_3 \cdot 9H_2O$, 98%) and Ruthenium(III) chloride ($RuCl_3$, 45-55%) were purchased from Aladdin Reagents Ltd. KOH (85%), The commercial Pt/C (20 wt%) catalyst and Nafion were purchased from Sigma-Aldrich. Ni foam (1.6 mm, ~95%) was used as received. Deionized (DI) water (18.3 MΩ) prepared all aqueous solutions.

1.2 Synthesis of $NiMoO_4$ NWs and Ru-dopped $NiMoO_4$ NWs

The method based on the literature was slightly modified, $NiMoO_4$ NWs were synthesized on NF [1]. Ultrasonic waves cleaned a commercial NF (1 × 2 cm^2) in 3 M hydrochloric acid solution, ethanol, and deionized water for 10 minutes each. After that, the NF, $Ni(NO_3)_2 \cdot 6H_2O$ (2.5 mM), $Na_2MoO_4 \cdot 2H_2O$ (2.5 mM), and 30 mL H_2O were placed into a polyphenyl-lined stainless-steel autoclave (50 mL). Then, sealed the reactor and placed it in an oven at 150°C for 6 hours. The resulting product was washed several times with deionized water and ethanol and dried for 12 hours. To synthesize Ru-doped $NiMoO_4$, 5 mg of $RuCl_3$ can be added during hydrothermal processes to produce Ru-$NiMoO_4$.

1.3 Synthesis of Ni/MoC@NC and RuNi/MoC@NC NWs

Ru-dopped $NiMoO_4$ NWs were carbonized on NF in a tube furnace to produce metal carbides. In a typical procedure, a $NiMoO_4$/NF piece was put downstream of

the tube furnace, and 0.5 g of DCD was placed 2 cm upstream. The system was heated to 500 °C at 2 °C min^{-1} under an inert gas atmosphere and cooled down after 2 h to obtain Ni/MoC@NC. For the fabrication of RuNi/MoC@NC NWs, Ru-$NiMoO_4$ NWs can be processed similarly to obtain RuNi/MoC@NC. By controlling the annealing temperature to 450℃ and 550℃, RuNi/MoC@NC-450℃ and RuNi/MoC@NC-550℃ are obtained, respectively. The mass loading of all the catalysts was about 2.0 ± 0.3 mg cm^{-2}.

1.4 Preparation Pt/C on NF

A Pt/C electrode was prepared by spraying ink of 40 mg 20% Pt/C and 60 μL Nafion onto the NF after sonicating it in a mixture solution of 540 μL ethanol and 400 μL deionized water for 30 min.

1.5 Preparation of NiFe LDH on NF

Based on previous literature [2], a piece of NF (1 × 2 cm^2) was immersed in a Teflon autoclave containing 15 mL deionized water with 0.3 mmol $Ni(NO_3)_2 \cdot 6H_2O$, 0.3 mmol $Fe(NO_3)_3 \cdot 9H_2O$ and 2 mmol urea. NiFe LDH was obtained by sealing the autoclave and heating it at 120 °C for 12 h. The sample was then washed several times with DI water and ethanol and dried. The loading amount of catalyst on NF was 2.4 mg cm^{-2}.

1.6 Physical characterizations

The micromorphological structure of the catalysts was characterized by SEM (JEOL 7500F) and TEM (JEOL JEM-2100F) equipped with energy-dispersive X-ray spectroscopy. A Thermo Jarrell Ash Trace Scan analyzer conducted ICP-OES. The

content of a specific element in the sample was measured three times, and the average value was obtained. The phases in each catalyst were detected using XRD on an Ultima IV with Cu Kα radiation. XPS (PHI 5300 ESCA system) was used to detect elements' types and valence states. Gas Chromatography (GC, Thermo Scientific TRACE 1300) can check the purity of the gas released from the two electrodes of the electrolyzer. The drainage method collects the hydrogen produced by electrolysis in the cathode chamber. A glass syringe (Hamilton Gastight 1002) was used to extract 1 mL of gas and inject it into the GC instrument.

1.7 Electrochemical measurements

Electrochemical measurements were conducted with a CHI 760E electrochemical analyzer (CH Instruments, Inc., Shanghai). The counter and reference electrodes of the three-electrode system were a graphite rod and a standard Hg/HgO electrode, respectively. Electrolytes were 1 M KOH and 1 M KOH + Seawater. The electrode size of different samples was about 1 cm^{-2}, and the immersed area in the electrolyte varies from 0.3 to 0.4 cm^{-2}. The mass of all catalysts loaded on NF was controlled at ~2 mg cm^{-2}. The sweep voltammetry (LSV) curves for all electrodes at a scan rate of 2 mV s^{-1} with 90% *iR* compensation. EIS was measured at a potential of 1.73 V (*vs*. RHE) from 0.1 Hz to 100 KHz with an amplitude of 5 mV. C_{dl} and ECSA values were obtained by plotting current density versus scan rate at 1.05 V (*vs*. RHE), where C_{dl} is half the slope of the line, ECSA = C_{dl}/C_s, and Cs is the specific capacitance. For the seawater splitting, the *iR* compensation was set to 90%. NiFe/MoC@NC/NF and RuNi/MoC@NC/NF were used as the anode and cathode, respectively. Stability tests were performed at a constant current density of 500 mA cm^{-2}. In addition, all experiments were performed at room temperature (~25 °C). An H-type electrolyzer with a diaphragm (30mm DuPont

117 ionic membrane) was used for electrolysis, and the cathode and anode gas chambers were strictly sealed except for the airway to produce pure gas.

1.8 TOF calculation

Eq. 1 is used to calculate the value of TOF [3]:

$$TOF = \frac{J \times A}{2Fm} \quad (1)$$

where J and A represent the current density ($C \cdot s^{-1} \cdot cm^{-2}$) and the surface area of the electrode (cm^2), respectively, F is the Faraday constant (96485 C mol^{-1}), m is the number of active sites (mole) and the factor 1/2 is the number of electrons required to produce 1 mol of H_2. The number of active sites is calculated by using Eq. 2.

$$m = \frac{Q}{2\mathrm{F}} \quad (2)$$

where Q is the charge (C) calculated by half-integration of the CV curve for the whole potential range measured in 0.1 M PBS (pH = 7). Thus, the number of exposed metal ion sites (m) for each electrocatalyst was estimated from integrated charge. Then TOF is calculated by normalizing the OER current density with the titrated active sites according to Eq. 1.

1.9 Theoretical calculations

VASP was used to conduct the DFT+U calculations [4, 5]. The plane wave basis set with a cutoff energy of 400 eV was used for both geometric optimization and single-point energy calculations. A generalized gradient approximation with the Perdew-Burke-Ernzerhof function was used to describe exchange-correlation interactions. For single energy calculation, gaussian smearing was employed with a σ value of 0.1 eV. The geometric convergence and electronic self-consistency thresholds were set at 0.05

eV/Å and 10^{-6} eV, respectively. All calculations do not consider spin, and the Brillouin region was sampled by a 3 × 3 × 1 γ-centered grid.

References

1. J. Zhang, T. Wang, P. Liu, Z. Liao, S. Liu, X. Zhuang, M. Chen, E. Zschech and X. Feng, *Nat Commun*, 2017, **8**, 15437.
2. J. Y. Chen, P. Y. Zhuang, Y. C. Ge, H. Chu, L. Y. Yao, Y. D. Cao, Z. Y. Wang, M. O. L. Chee, P. Dong, J. F. Shen, M. X. Ye and P. M. Ajayan, *Adv Funct Mater*, 2019, **29**, 1903875.
3. L. B. Wu, L. Yu, F. H. Zhang, B. McElhenny, D. Luo, A. Karim, S. Chen and Z. F. Ren, *Adv Funct Mater*, 2021, **31**, 2006484.
4. J. Hafner, 2008, **29**, 2044-2078.
5. P. L. Silvestrelli, *Phys Rev Lett*, 2008, **100**, 053002.

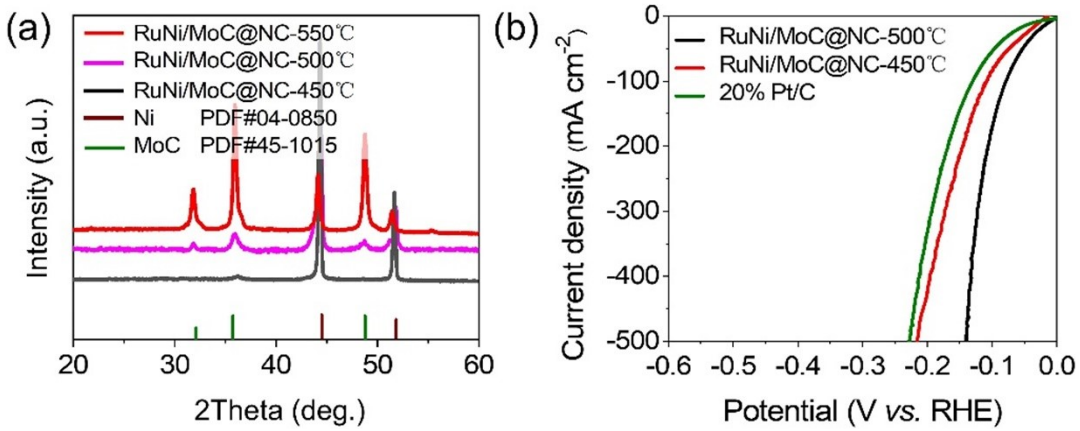

Fig. S1. (a) The XRD patterns of RuNi/MoC@NC-450℃, RuNi/MoC@NC-500℃ and RuNi/MoC@NC-550℃. (b) The LSV polarization curves of the catalysts in 1 M KOH for HER.

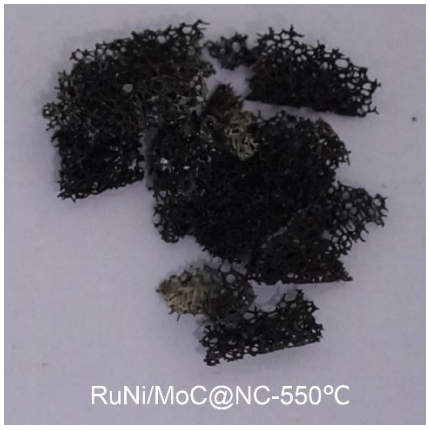

Fig. S2. The digital photo of RuNi/MoC@NC-550℃.

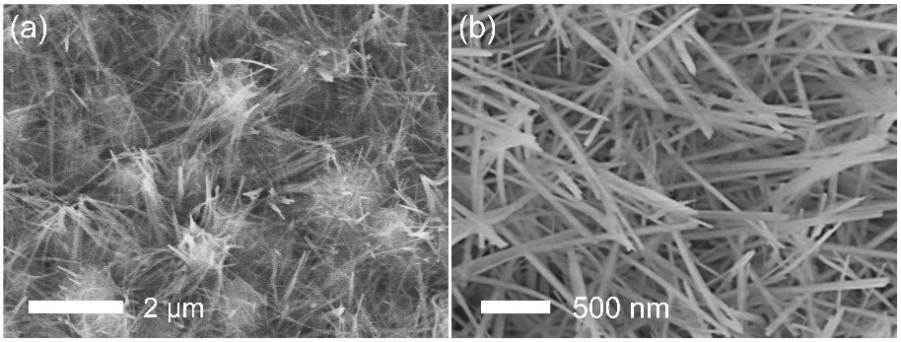

Fig. S3. SEM images of $NiMoO_4$ at different magnifications.

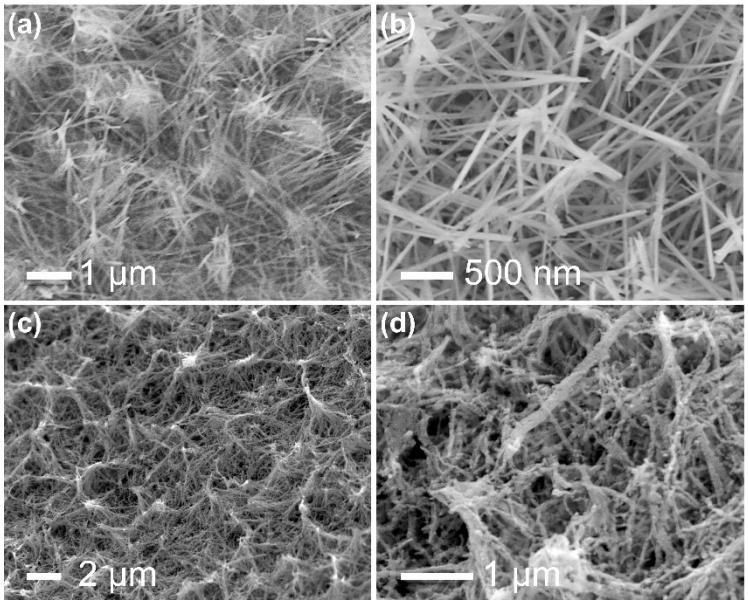

Fig. S4. SEM images of (a-b) Ru-$NiMoO_4$ precursor and (c-d) Ni/MoC@NC in different magnifications.

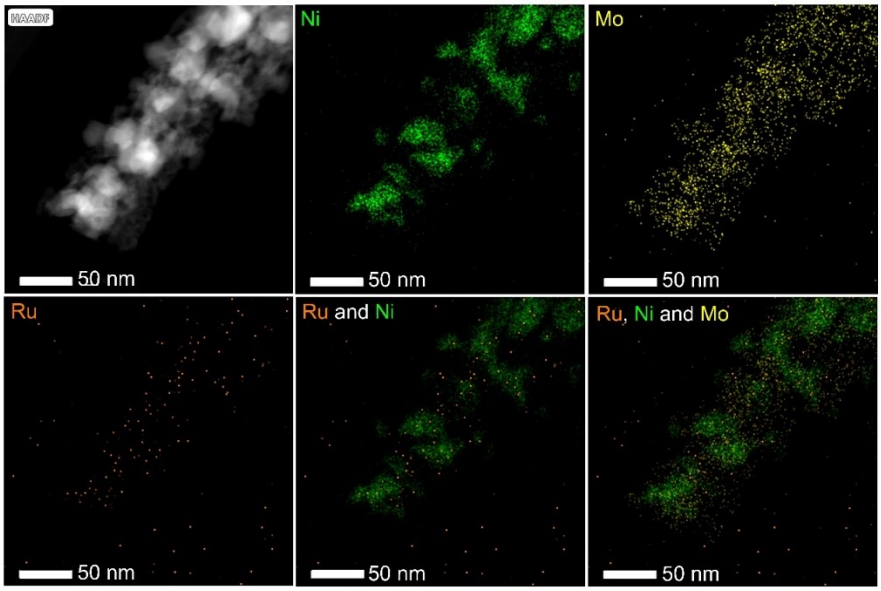

Fig. S5. The element mapping images of Ni, Ru, and Mo are superimposed.

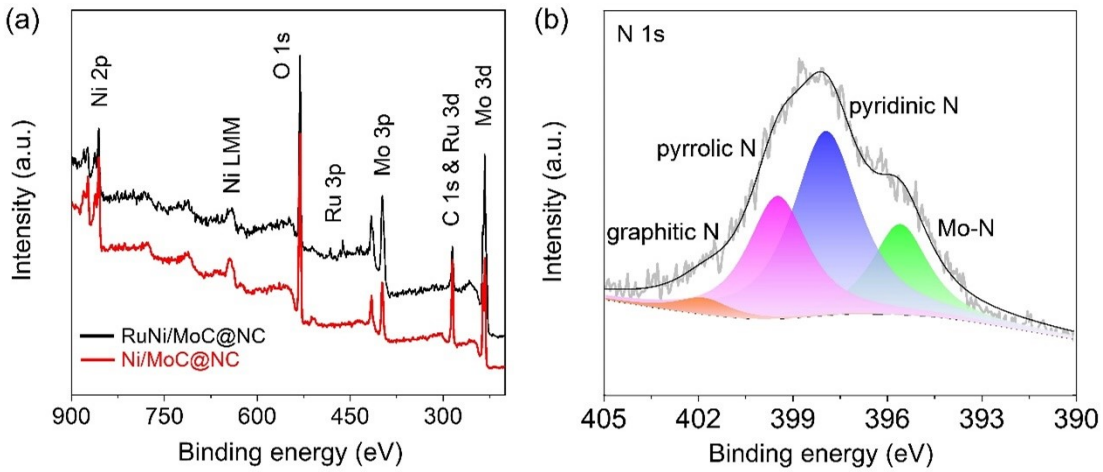

Fig. S6. (a) Full of XPS survey spectra of RuNi/MoC@NC and Ni/MoC@NC. (b) The high-resolution XPS spectra of N 1s of RuNi/MoC@NC.

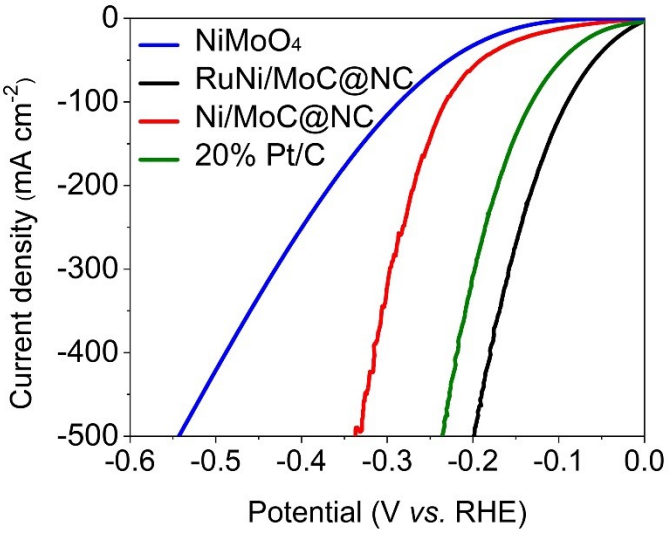

28

29 **Fig. S7.** LSV polarization curves of the catalysts without *iR* compensation in 1 M KOH

30 for HER.

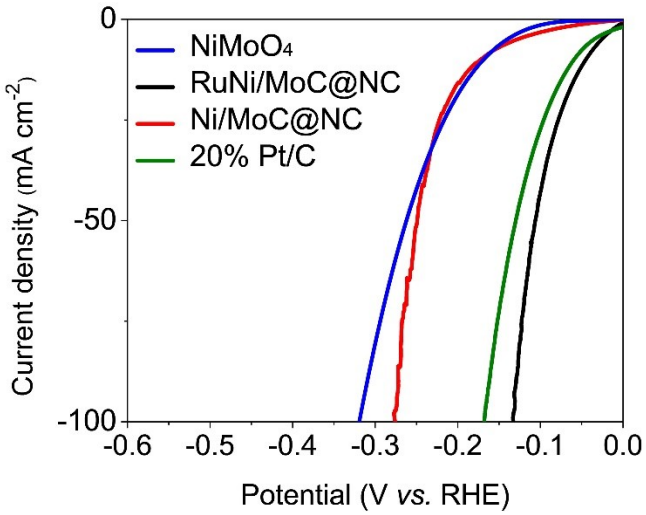

Fig. S8. The mass activity of Pt/C, $NiMoO_4$, Ni/MoC@NC, and RuNi/MoC@NC for HER.

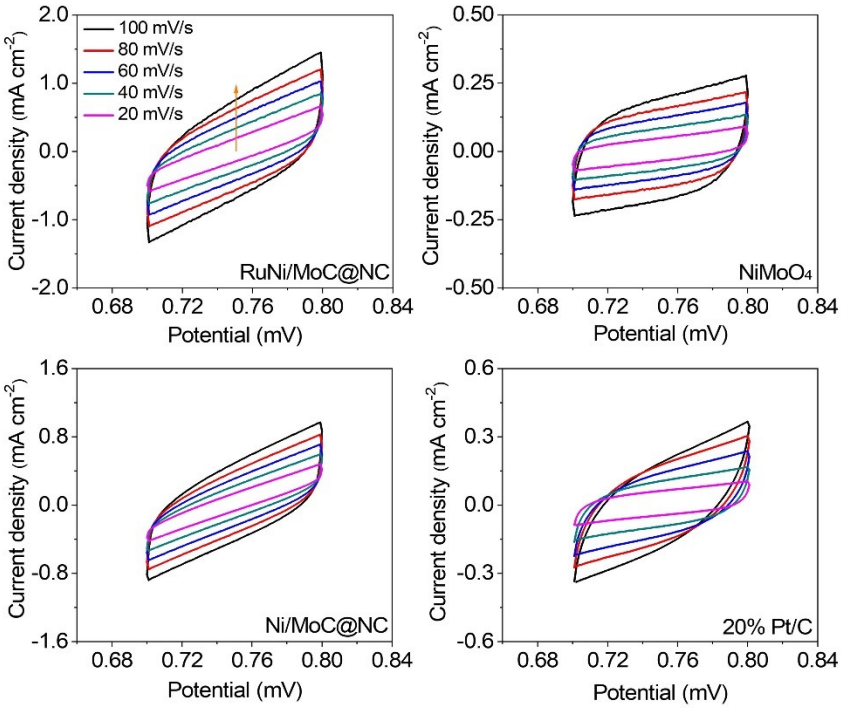

Fig. S9. The CV curves of different sweep speeds of the prepared catalysts.

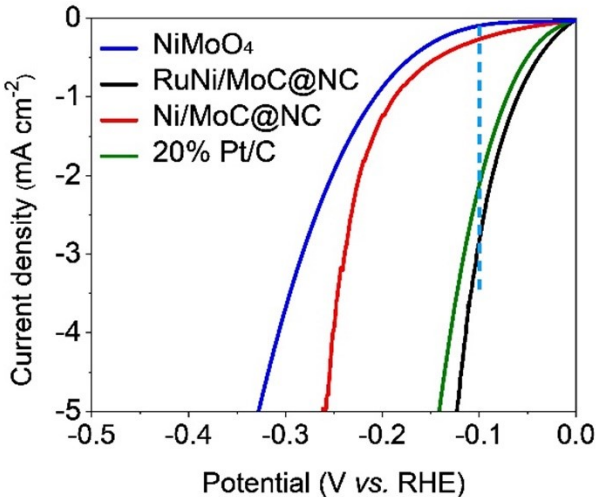

Fig. S10. The TOF plots for the RuNi/MoC@NC, Ni/MoC@NC, $NiMoO_4$, and 20 wt% commercial Pt/C in 1 M KOH.

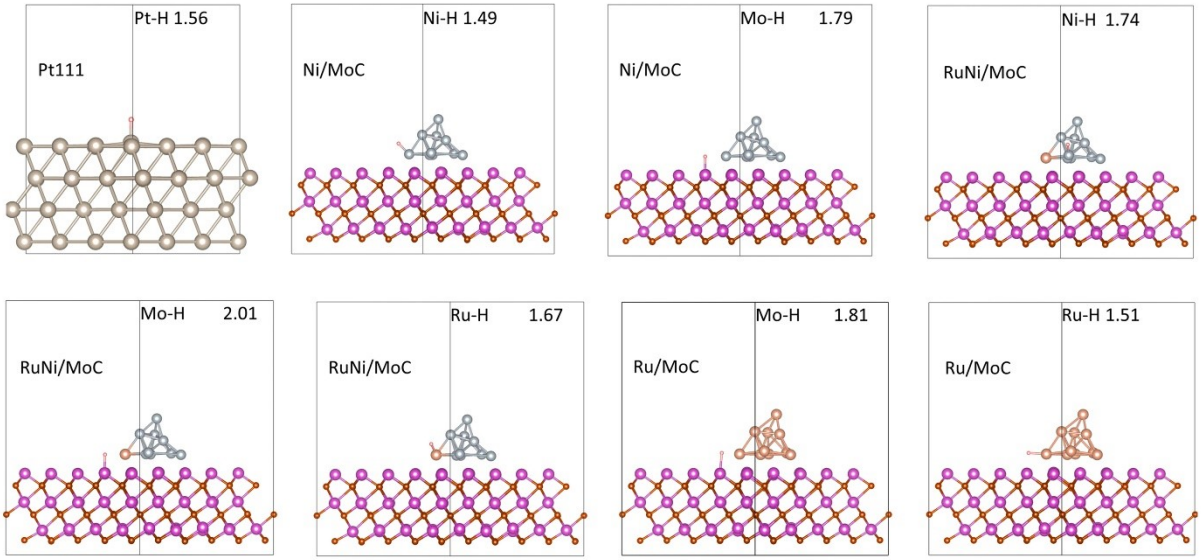

Fig. S11. Adsorption models of hydrogen atoms at different adsorption sites on Pt (111) slab, Ni/MoC, RuNi/MoC and Ru/MoC surfaces, where gold yellow, silver, pink, orange, and white spheres represent Ru, Ni, Mo, C, and H atoms, respectively.

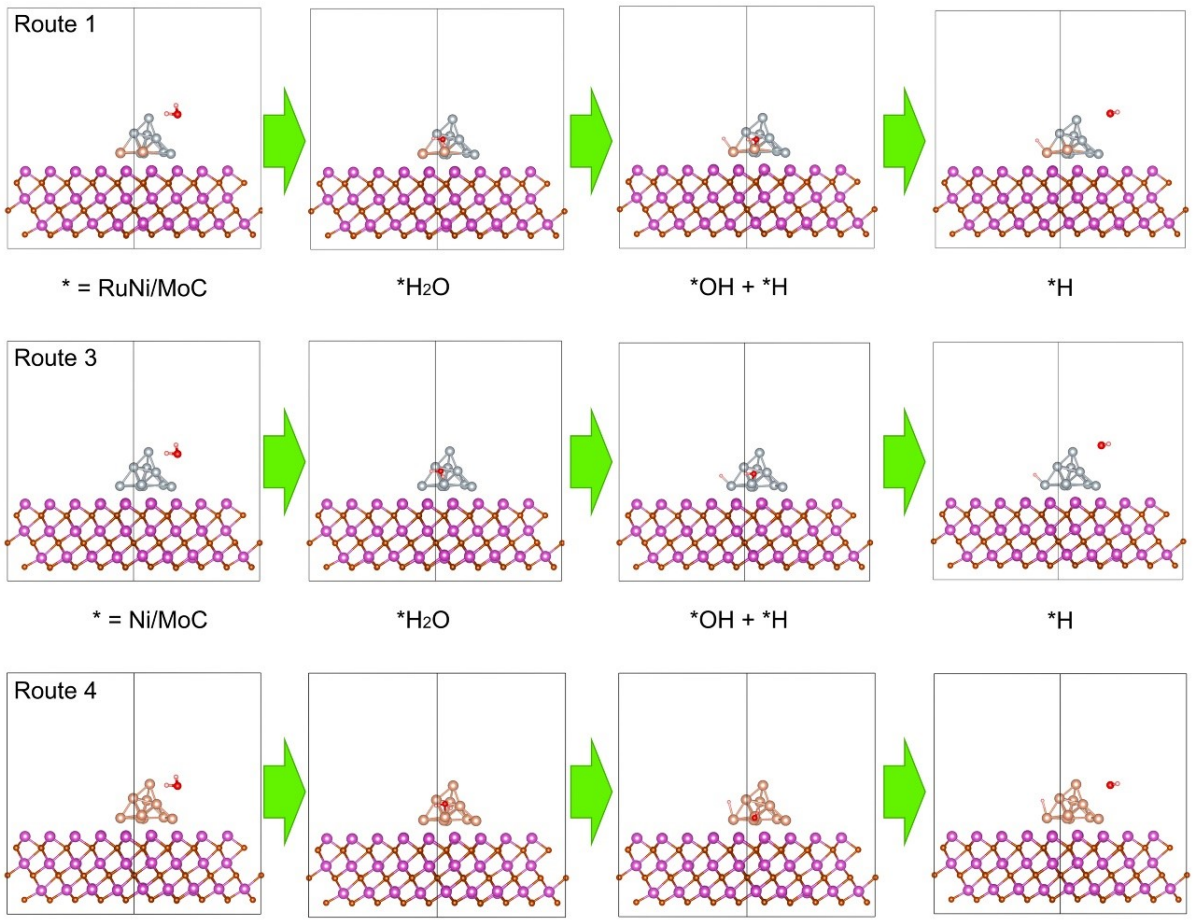

Fig. S12. Atomic configurations of optimized Ni/MoC, RuNi/MoC and Ru/MoC heterojunction and its corresponding alkaline HER intermediates, where gold yellow, silver, pink, orange, red, and white spheres represent Ru, Ni, Mo, C, O, and H atoms, respectively. (Route 1: Cooperative catalysis between Ru atoms in RuNi/MoC; Route 3: Cooperative catalysis between Ni atoms in Ni/MoC; Route 4: Cooperative catalysis between Ru atoms in Ru/MoC)

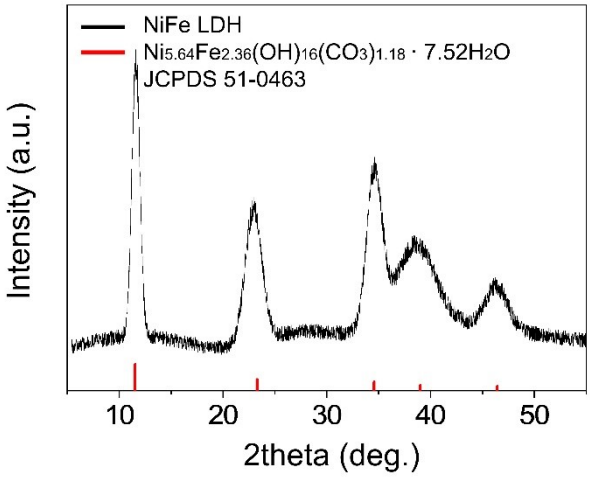

Fig. S13. The XRD pattern of the prepared NiFe LDH.

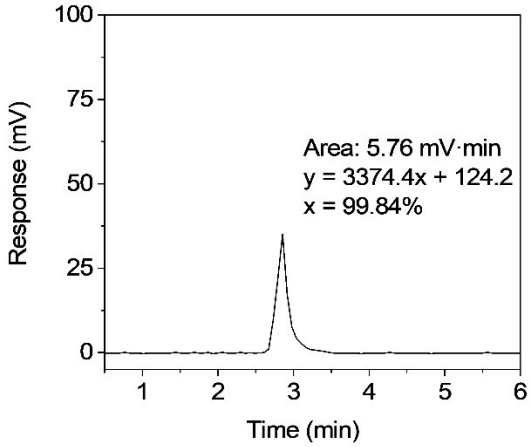

Fig. S14. Measuring the farad efficiency of the electrolyzer by drainage method in alkaline seawater.

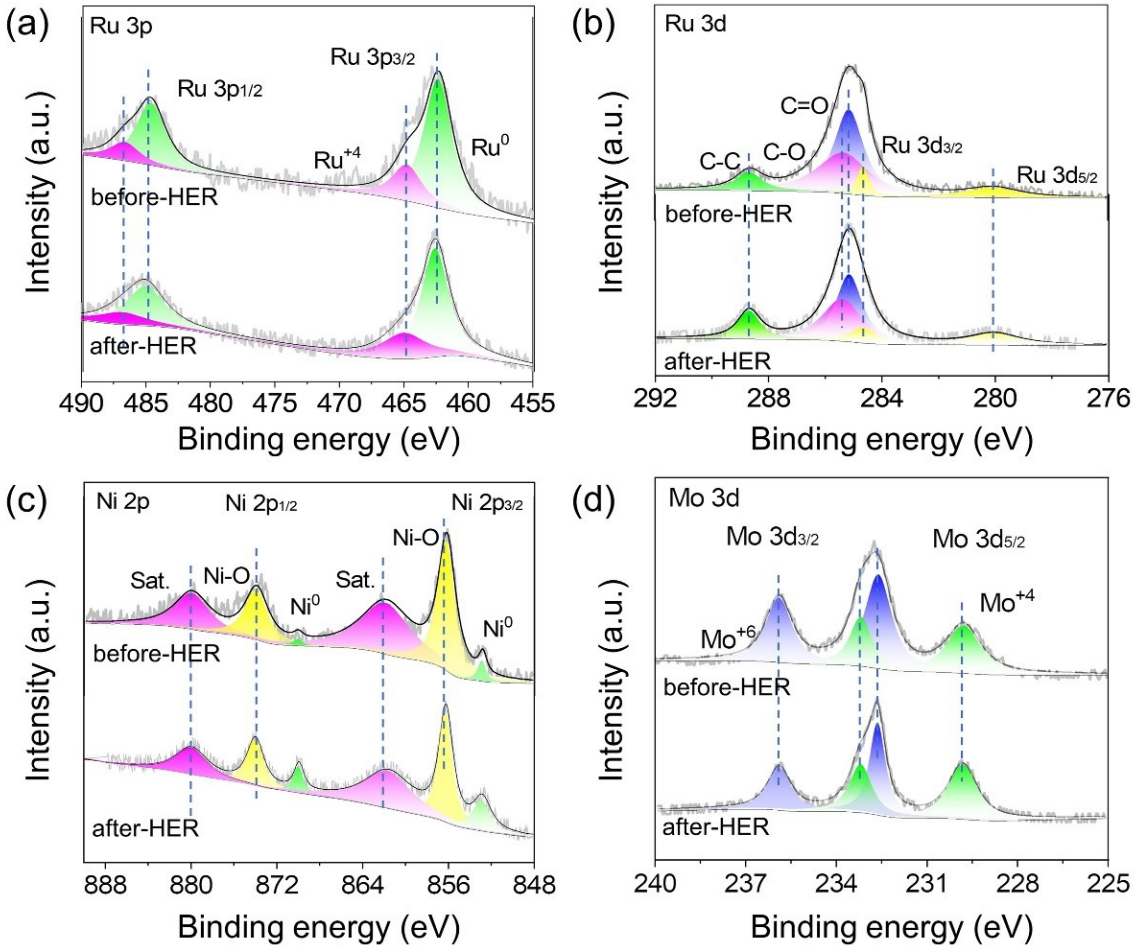

Fig. S15. The high-resolution XPS of (a) Ru 3p, (b) Ru 3d, (c) Ni 2p, and(d) Mo 3d of the catalyst before and after the stability test.

Table S1. The ratios of Ru-$NiMoO_4$ and RuNi/MoC@NC were determined by ICP-OES spectroscopy.

Catalyst	Ru-$NiMoO_4$	RuNi/MoC@NC
The atomic ratio of Ru to Ni	1:11.92	1:12.45
The content of Ru (wt%)		~3.72%

Table S2. Comparison of HER catalytic performance in 1 M KOH between RuNi/MoC@NC and recently reported self-supported catalysts.

Catalyst	Support	η_{100} (mV)	Reference
RuNi/MoC@NC	Ni foam	78	This work
$(Fe_{0.74}Co_{0.26})2P/Ni_3N$	Ni foam	113	Small, 2023, 2207082
FeNiP-NPHC	Ni foam	180	Adv. Funct. Mater., 2022, 32, 2205767
MnCoNiSe	Ni foam	*122	Applied Catalysis B: Environmental, 325 (2023) 122355
$Ni/Ni(OH)_2$	Ni foam	*142	J. Mater. Chem. A, 2022, 10, 21848
$NiCoHPi@Ni_3N$	Ni foam	174	ACS Appl. Mater. Interfaces, 2022, 14, 22061−22070
NiFeS	Ni foam	196	J. Mater. Chem. A, 2023, 11, 1116

* Value calculated from the curve shown in the reference.

Table S3. The values of the *Rs*, R_{ct} and CPE of the catalysts.

Catalyst	*Rs* (Ω)	R_{ct} (Ω)	*CPE, Yo* (S·sec^n)	*Freq power, n (0<n<1)*
Ni/MoC@NC	0.074	0.55	1.25	0.8304
RuNi/MoC@NC	0.072	0.73	0.94	0.8296
Pt/C	0.068	0.91	0.75	0.8321
$NiMoO_4$	0.079	1.09	0.63	0.8286

Table S4. Some atoms' valence electrons are obtained by calculating the Bader charge.

Atomic species	RuNi/MoC				Ni/MoC		
	Ru	Ni	Mo	C	Ni	Mo	C
The average number of valence electrons	8.45	10.13	5.01	4.95	10.15	5.03	4.95

Table S5. Comparison of electrochemical performances for full water splitting in 1 M KOH + seawater.

Catalysts	η_{100} **(V)**	**Reference**
NiFe LDH|| RuNi/MoC@NC	1.58	This work
S-(Ni, Fe)OOH||NiMoN	1.62	Energy Environ. Sci. 2020, 13, 3439-3446
CoP_x@FeOOH||CoP_x	1.71	Appl. Catal., B 2021, 294, 120256
Ni_3S_2-MoS_2-Ni_3S_2||Ni_3S_2-MoS_2-Ni_3S_2	1.80	Electrochim. Acta 2021, 390, 138833
Go@Fe@NiCo||Go@Fe@NiCo	*1.80	J. Mater. Chem. A 2020, 8, 24501-24514
S, P-(Ni, Mo, Fe)OOH/NiMoP||S, P(Ni, Mo, Fe)OOH/NiMoP	1.861	Appl. Catal., B 2021, 293, 120215
NiCoHPi@Ni_3N||NiCoHPi@Ni_3N	1.86	ACS Appl. Mater. Inter. 2022, 14, 22061-22070

***** Value calculated from the curve shown in the reference.

Table S6. The ratios of RuNi/MoC@NC (post-HER) were determined by ICP-OES spectroscopy.

Catalyst	RuNi/MoC@NC
The atomic ratio of Ru to Ni	1:12.61
The content of Ru (wt%)	~3.64%